How to Analyze, Preserve, and Communicate Leonardo's Drawing? A Solution to Visualize in RTR Fine Art Graphics Established from “the Best Sense”

How to analyze, preserve, and communicate Leonardo's drawing? A solution to visualize in RTR fine art graphics established from "the best sense" *

Fabrizio Ivan Apollonio†, Riccardo Foschi†, Marco Gaiani†, Simone Garagnani†

†Dept. of Architecture, Alma Mater Studiorum University of Bologna, Bologna, Italy, fabrizio.apollonio, riccardo.foschi2, marco.gaiani, simone.garagnani@unibo.it

ABSTRACT

Original hand drawings by Leonardo are astonishing collections of knowledge, superb representations of the artist's way of working, which proves the technical and cultural peak of the Renaissance era. However, due to their delicate and fragile nature, they are hard to manipulate and compulsory to preserve. This work presents the outcomes of a ten years long research program, in which a complete workflow was developed to produce a novel system designed to replace, investigate, describe and communicate ancient fine drawings through what Leonardo calls "*the best sense*" (i.e. the view). *ISLe* (*InSightLeonardo*), targeted to a possible wide audience made of museums' visitors, art historians but also, and most importantly, scholars and conservators–restorers, is a comprehensive process, ending in a customized visualization app, meant to acquire drawings and translate them into digital replicas, following principles whose main directives are *realism* (accurate shapes and surfaces representation) and *responsiveness* (models change their appearance when directly manipulated by observers). This paper introduces the appearance modeling with the aim of an accurate RTR used. After a general introduction of the cultural context in which those drawings were authored, in section 2 of this paper, the *ISLe* system is extensively described. Section 3 introduces features proper of materials to be modeled and rendered, namely paper, iron-gall ink, stylus, and metalpoint. Section 4 describes the solutions adopted to model materials while section 5 introduces an evaluation of their rendering solution. The concluding remarks are presented in section 6.

CCS CONCEPTS

• **Applied computing~Arts and humanities~Media arts** • Information systems~Information retrieval~Document representation • Computing methodologies~Computer graphics~ Reflectance modeling

KEYWORDS

3D digital artifact capture, analytic tools for scholars, Leonardo da Vinci, Renaissance drawings, Color reproduction, Real-Time Rendering, Shaders, Material classification, and reproduction.

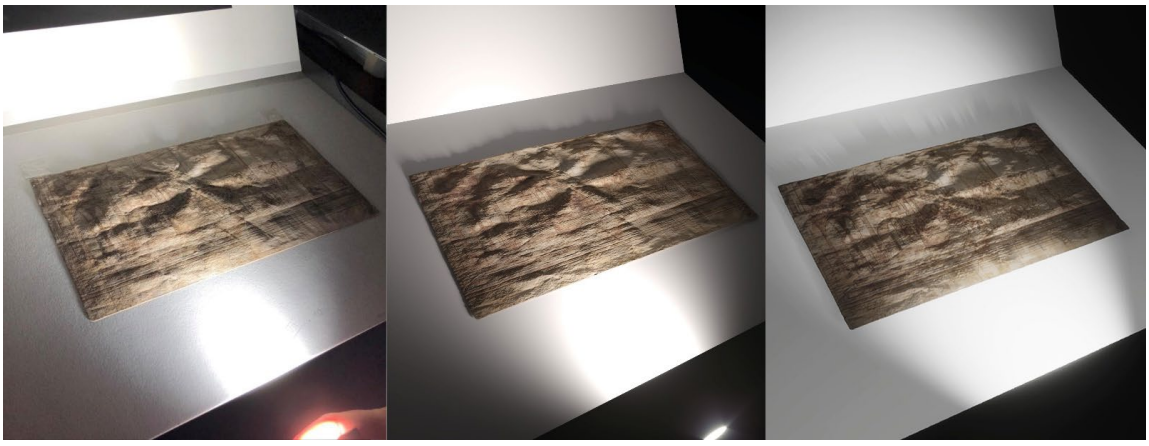

Figure 1: Leonardo's *Study of various buildings in perspective:* comparison between real drawing (left) and a virtual model with similar raking light source and our material reconstruction rendered with Corona render (middle) and our rendering system (right).

1 Introduction

The first known drawing by Leonardo da Vinci is the *Landscape 1473*, preserved at the Cabinet of Drawings and Prints of the Uffizi in Florence (GDSU), made when Leonardo, twenty-one years old, was still at the workshop of Andrea del Verrocchio, and dated by himself "on the [feast] of Saint Mary of the Snow, on the day of August 5, 1473". The best definition of the drawing is by Martin Kemp gives: "It is simply the first dated landscape study in the history of Western art" [1]. It is a seemingly simple artwork, roughly the size of an A4 sheet (exactly 194 x 285 mm). We know well only the face bearing the landscape drawn in pen, which has always been considered the result of a unitary composition. However, the drawing also features a back, almost completely unknown. Its small size then makes it difficult to understand both to the simple visitor of an exhibition, and to the expert who, for safety reasons, can only observe it within its passe-partout, at a distance of at least 80 cm and one side at a time. The careful observation of the drawing, however, shows incredible surprises, starting with the paper that suggests that the landscape is not the main subject of the sheet, but Leonardo's drawing born after a first trial on the rear face then discarded. The paper features are imperceptible in an overall observation, but clearly distinguishable in the enlarged detail, which shows how the wire rods, while the back is smooth and well-treated, signifying that this is the main side of the paper sheet. The drawing then, at a closer look, shows more instruments to trace signs: lead point, four types of iron-gallic ink, red chalk, white gouache, and several types of signs over-imposed, not only by Leonardo but also by other owners/collectors over time.

The accurate identification of these features is today achieved using multispectral imaging, presenting the main advantage to be non-invasive/non-destructive. Different spectra enable a precise examination and identification of colors and pigments, the visualization of underlying features, and the identification of varying materials or surface conditions, allowing important advances on the attribution of drawings and information on their technique [2]. However, this approach presents some shortcomings for the restorer:

the absence of geometrical surface information (it could be provided by the laser scanning micro profiling technique but is complex and not completely safe);

the complexity in the adoption of many, different and highly specialized analysis;

the limited user-friendliness of acquisition tools and viewer systems, which require exceptional user efforts to cross data from the different analyses.

These observations, along with the rule requiring not to exhibit them for more than three months every three years, well describe the difficulty of analyzing, conserving, and exhibiting the ancient drawings.

To overcome these problems since 2010 our group, following suggestions by Marzia Faietti, at the time director of the GDSU, developed a different type of solution. A new system was designed to replace, investigate, describe, and communicate ancient fine drawings through what Leonardo calls "the best sense" (i.e. the view). It exploits the interplay of changing light directions and points of view directions to allow an examiner to visually explore and understand the characteristics of a surface, a task at which a researcher or conservator–restorer is trained to.

From a technical perspective, this means to give a rich representation of real surfaces, reproducing accurately surface topography, appearance and accurate rendering of colors, to enable the tracing and hatching investigation that corresponds to the possibility of reconstructing the artist's method, as well as the superimposed sediments and conservation interventions during the time.

The solution allows us to safely acquire, digitally reconstruct in 3D, and visualize in high-quality Real-Time Rendering (RTR) the ancient drawing with high color fidelity and resolution (imperceptible difference to the expert observer's view), ensuring the whole shape and surface reflectance quality. It is based on two paradigms: 'drawing as in your hands' and 'showing what you don't see'. It can be used both by the conservator on desktop PCs or tablets, as well as by visitors to an exhibition using high-resolution large size monitor and a touch interaction suitable based on the same gestures of use of smartphones.

The system is in the same line of other solutions addressing the same problems and approach, e.g. [3, 4], with the first one it shares the main two properties of the images produced by the system:

realistic, accurately representing the shapes and material properties of surfaces;

responsive, changing appearance suitably with direct manipulation and changes in observer viewpoint.

Differently, from previous approaches, our solution exploits commercial hardware, is based on low-cost and open-source software customized for the rendering runtime, and our software for the acquisition phase, which is open-source for the institutions. For conservators and restorers, the solution allows us to improve vision through the non-invasive examination of artworks, in order to monitor the effects of conservation interventions and to quickly cross information, from multiple and different sources, and difficult to superimpose. During an exhibition, it can be combined with the original artwork to allow it to be 'read' or as its substitute.

Even though the application was developed using Leonardo drawing, the so-called *ISLe* (*InSightLeonardo*), could be easily used to show the works of the other artists between the 15th and 17th centuries, since the features of Leonardo's drawings are still the most expensive about all the main parameters of acquisition and rendering, as shown by an investigation we carried out in 2010 [5], and they include also writing.

A first naïve solution was presented in 2015 [6] but in the last three years, the whole visualization system was completely rebuilt, with many improvements allowing a superior rendering quality. This progress not only implies new technical solutions, but it mainly introduces better model's appearance exploiting the experience coming from five Leonardo's drawings acquisition and analysis, namely:

- Leonardo da Vinci, *Landscape, 1473*, recto: pen and iron-gall inks, lead point, blind point on paper; verso: pen, iron-gall inks, black, and red chalk, lead point, blind point on paper, 194 x 285 mm, Florence, Le Gallerie degli Uffizi, GDSU, inv. 8P
- Leonardo da Vinci, *Study of various buildings in perspective (study for the background of the Adoration of the Magi)*, around 1481, metal point, reworked with Pen and iron-gall ink, diluted iron-gall brush and ink, partially oxidized white gouache highlights (basic lead carbonate), stylus and compass on light brown prepared paper, 164 x 290 mm, Florence, Le Gallerie degli Uffizi, GDSU, inv. 436 E
- Leonardo da Vinci, *Study of proportions of the human body known as The Vitruvian Man*, around 1490, metal point, pen, and iron-gall ink, watercolor ink touches, stylus on white paper, 345 x 246 mm, Venice, Gallerie dell'Accademia, Gabinetto dei Disegni e delle Stampe, inv. 228
- Leonardo da Vinci, *Two mortars launching explosives*, around 1485 (or shortly after), traces of black pencil (?), stylus tip, pen, and iron-gall ink, diluted ink and watercolor with reworking on the right side, 219 x 410 mm, Milan, Veneranda Biblioteca Ambrosiana, Codex Atlanticus, f. 33
- Leonardo da Vinci, *Fortress with a square plan, with very high scarp wall and concentric layout, with corner towers and grandiose ravelin in front*, 1507 or later, pen and iron-gall ink on black pencil, 131-207 x 436 mm, Milan, Veneranda Biblioteca Ambrosiana, Codex Atlanticus, f. 117

While we refer to the 2015 article [6] for an overview of the system and to another work of 2019 [7] for a general description of the system, in this paper we focus on the appearance modeling with the aim of an accurate RTR. This visualization stage introduces peculiar needs since the original drawings digitally acquired had to be precisely replicated in a comprehensive visual framework, meant to mimic real behaviors of metalpoints, inks and papers toward the light. Moreover, one of the purposes of our research was typically the development of 3D models aimed at scholars, whose needs of flexible visualization and custom exploration require the use of an accurate physically-based render engine. A visual example of results from our solution is in Figure 1 where the drawing *Study of various buildings in perspective* illuminated with a raked light in a real view is placed next to a synthetic image done with the physically-based renderer Corona Render and to the *ISLe* visualization. The light position and intensity and the boundary conditions of the virtual scene are measured from the real scene to ensure a proper comparison. In section 2 the *ISLe* system is depicted. Section 3 introduces materials features to be modeled and rendered, namely paper, iron-gallic ink, stylus and metalpoint. Section 4 describes the material modeling solution. Section 5 presents an evaluation of the rendering solution. The concluding remarks are presented in section 6.

The *ISLe* system

The *ISLe* system was developed to visualize surrogates of ancient drawings through their view, to manipulate them using usual gestures, to investigate them through typical tools such as enlarged and all directions views, to explore front and back of drawings with a simple rotation of the paper sheet 'as in the hand' and different

types of illumination (zenithal, raking, ...). Overall, from the point of view of visual analysis, the topic addressed is the perceptually indistinguishable visualization of the digital from the original drawing, exploiting a high-resolution monitor and with full sRGB-IEC 61966-2-1 color space support. The sRGB space was selected because it presents full support of 3D API graphics used while the potential issues (non-linearity, smaller amplitude of the human perceived color space) do not affect the quality of *ISLe* due to the absence in the drawings considered of poorly represented colors. Iron-gallic ink, black chalk, red chalk, and paper have colors inscribed in the sRGB color space, without the need for color clipping or remapping.
The perceptual visualization of a drawing underlies three specific issues to which the application must be able to provide an answer to:

- the evaluation of subtle color differences (i.e. the colorimetric analysis);
- the quality and consistency assessment of the sign;
- the interaction with the total appearance of the drawing [8].

The first requirement is not particularly difficult to achieve, considering the tonal range amplitude to be acquired and reproduced since the number of colors in the drawings is very limited, but complexities are in the modeling of the various materials reflections (paper, ink, chalk, metal point*, biacca*), and in the rendering of paper grain and sign paths. Since the RTR of a surface reflection requires strong simplifications of the physical behavior of light and its interactions with the surface in order to be computable in a short time, the goal of *ISLe* was set in returning at least perceptual fidelity of color. The second requirement is stronger due to the extremely subtle sign that Leonardo is capable of. Measurements carried out on several drawings, but especially on the famous *Study of a female face* (Le Gallerie degli Uffizi, GDSU, Florence, inv. 428 E) show values of the signs at a minimum of 90 μm thick, that is, very close to that limit of visual contrast sensitivity for the lighting that Leonardo used during their drafting [9].
ISLe provides a solution to these requirements and allows precise estimations of the drawings surface properties. In particular, it correctly shows the depth information (the typical thicknesses left by pens and pencils rarely exceed 10 μm, with an average of 5 μm; the paper micro-grain has bumps not exceeding 100 μm), and accurately returns the reflectance of the surface, which is fundamental to accurately perceive the drawing. *ISLe* workflow is based on five modules:

1. accurate and safe on-site 48-bit at each pixel location color capture, using imaging techniques able to guarantee color fidelity, absence of lighting falls on the whole image and appropriate resolution;
2. accurate fully automated Color Correction (CC) from RAW images to reproduction on the final display device based on our software SHAFT (SAT & HUE Adaptive Fine Tuning) [10];
3. correct appearance modeling of the paper, ink, chalk, and metalpoint, to faithfully reproduce the drawing surface features in the RTR visualization window;
4. high-fidelity RTR of the total appearance of the drawing at a resolution of 50 μm, and an accurate color reproduction using an RTR engine portable on multiple devices (*wall*, PC monitors, *touch* table*, tablet, smartphones*);
5. visualization and navigation interface based on an adaptation of the traditional multitouch interaction paradigm to fit the exploration of 2D-3D contents to minimize uncommon gestures.

2 Leonardo's drawing tools and materials

Many studies in the last ten years focused on drawing aim, features, media, and techniques from 14th century to the end of 16th [11, 12] and, in particular, techniques and features at Leonardo's time are well investigated and that's why they were a solid reference for our work [13, 14]. Moreover, the Cennino Cennini's *Il libro dell'arte* [15] is particularly important for the understanding of fifteenth-century Italian practice. This treatise gives very practical advice on creating drawings and paintings and was known also in the Andrea del Verrocchio atelier, as well as by the young Leonardo. We will mainly refer to these sources to correctly understand and model techniques, tools and instruments used by Leonardo.
We will focus on metalpoint, black chalk and ink that are the most common media used by Leonardo and that we met on the analyzed drawings.

2.1 Paper

The entirety of Leonardo's extent graphic work is on paper, mostly ranging in size in the area that we could summarize from today known A5 to A3 format. The five drawings examined range from 164 x 290 mm to 219 x 410 mm. Most of the Leonardo drawings are executed on very fine quality paper, made from high-grade white fibers, well beaten and evenly distributed with a well-pressed finish, ideal for fine pen and ink drawing [16]. This high-quality paper contains fewer impurities, generally resulting in a finer, smoother finish. Surface texture is significantly affected by the formation, drying and pressing processes involved in papermaking. Sometimes the wire structure of the sheet, in the form of laid and chain lines, might be very pronounced and create a pattern that is clearly visible even without the use of transmitted light. A clear difference between the two sides of the paper can be often observed with the naked eye, as in the *Vitruvian Man*. Papers used by Leonardo had chain lines from 22-25 to 23-26 mm apart with 10-14 laid lines per centimeter. Due to the production process, the paper sheets present variable thicknesses. In our knowledge paper thickness was measured for two Leonardo's drawing, the *Vitruvian Man* [17] and the *Possible Self-Portrait* [18]. The mean paper thickness measured using a caliper and a paper-gauging micrometer, ranges from 75 to 200 μm, but the higher measurement is affected by the paper treatment meant to support silverpoint and the accuracy of the measurement instrument.

The appearance of a typical sheet of paper is a function of its detailed structure, the presence and concentration of light-absorbing groups, the refractive indices of its components, its basis weight, and its surface reflective characteristics [19]. Issues related to the presence of contrasting fibers and formation uniformity also affect the appearance of paper. Paper's optical characteristics and their measurement have been described in many reviews and textbooks, recently in [20], which was our reference in our work.

The paper appears white due to the scattering and reflecting effect caused by the fibers. When light strikes paper, the light is either reflected (known as specular reflection or gloss), transmitted, scattered, or absorbed. A high light scattering coefficient, contributing toward the opacity of paper products, tends to be favored by a bulky structure. Main parameters featuring paper are then:

- Diffuse reflectance (i.e. the albedo)
- Opacity (ability to hide whatever is printed on its backside or subsequent sheets)
- Gloss
- Formation uniformity (local variations in the opacity, a phenomenon resulting from non-uniform distribution of fibers within the plane of the sheet and non-uniform thickness of the sheet)
- Transmission
- Scattering and absorption in which the void spaces of the paper play an important role.

Next, we review the main parameters of paper.

2.1.1 Roughness and gloss

Two parameters frequently used in the current paper fabrication industry allowed us to better define the paper appearance behavior: the roughness and the gloss.

Gloss can be described as the relative ability of the paper to reflect light at a mirror angle. The gloss of the paper could be attributed mainly to the mirror-like nature of its surface microstructure, originating in sub-surface reflection or scattering of light. Image analysis methods have used to characterize gloss uniformity over a wide range of dimensions at the microscale (<100 μm) [21].

Roughness is a good indication of surface texture and irregularities from mesoscale features (e.g. poor fiber dispersion) and microscale features (e.g. particle size distribution) [22] and is usually measured using a profilometer. In our case, point by point, the roughness was mapped using an image-based method photometric stereo technique [23], allowing to recover the 3D shape of an object by taking multiple images at the fixed view but varies lighting positions.

Various approaches have been proposed to capture the angular appearance variation of fine art surfaces (e.g. [24]), usually represented by a Spatially Varying Bidirectional Reflection Distribution Function (SVBRDF), describing the relation between incoming irradiance and the outgoing (reflected) radiance for every point on a surface. Several approaches employ sparse sampling using point light sources (e.g. [25]), however, the specular reflectance is not separately modeled or becomes noisy. As a solution, surfaces are sorted into

material groups, and the angular measurements are combined within each group and shared across the spatial domain (e.g. [26]). In our case this approach is feasible, exploiting an accurate segmentation of materials based on a supervised feed-forward neural network [27] consisting of 10 intermediate layers in addition to the input and output layers. The learning algorithm used is the Levenberg-Marquardt backpropagation [28], for its performance characteristics. The results were gloss maps for each material.
The most common procedure for the sparse measurement uses a gloss meter or a spectrometer evaluating the specular/diffuse reflectance ratio. JIS 8741 and Tappi T 480 standards give a consistent measurement mode. In our case, the solution comes from the observation that fine art drawing rendering requires a spatial resolution of at least 600 dpi (43 μm). These spatial resolution methods based on angular measurements are very time-consuming in terms of data acquisition and processing (i.e. due to their angular resolution), limiting their practical use for reproducing whole drawings. In our approach we can suffice with only a gloss parameter, representing the magnitude of the specular reflectance peak evaluated pixel by pixel using photometric stereo techniques and producing a gloss map for each pixel sampled.

2.1.2 Scattering and Absorption of Light

To evaluate reflectance characteristics and opacity of non-glossy paper with reasonable accuracy, for many years it was used a set of equations derived by Kubelka and Munk [29] in which the layered material is envisioned as being uniform, isotropic, non-fluorescent, and nonglossy. Using Kubelka-Munk equations inconsistencies were found for real paper samples in the case of sensible paper's non-uniformity at a submicroscopic level (that is the case of Leonardo paper). To minimize these problems an alternative approach was developed based on the work of Stokes [30]. This solution, however, presents the practical drawback of the general lack of the parameters in the equations in the literature.
To improve accuracy and realism of optical analyses an approach based on three-dimensional radiative transfer theory was proposed in [31], showing good agreement with the Mie theory, which takes a detailed approach to determine optical properties, based on microstructure. In our case, we improve on this direction exploiting the work of [32] that, starting from image-based measurements, models the paper as a highly scattering, optically thick material, with a combination of subsurface scattering, specular reflection, retro-reflection, surface sheen, absorption, and transmission.
A key step to use this method is to find a correct refraction index of paper, which specifies the resistance under which light passes through the material. The refraction index of the Leonardo drawing *Possible Self-Portrait* was measured and reported for many frequencies [33] and was used in our solution taking as reference the value for a wavelength of 589.3 nm that is ~1,66.

2.2 Metalpoint and black chalk

The first approach of the artist with the empty paper sheet is with a medium leaving the ability of easy correction and erase the wrong signs. In the case of Leonardo, these drawing instruments consist of metalpoints and black chalk.

2.2.1 Metalpoint

The term 'metalpoint' refers to both the drawing tool and the technique to produce fine lines with little texture. A metalpoint is a slender stylus made from a soft metal that leaves a mark greyish, relatively light, and with little texture. A simple blind stylus, instead, merely produces an indented line. Increasing the pressure does not tend to give a darker line, and there is little flexibility within lines, with shading built up through a series of strokes rather than a variation of width [12]. Metalpoint marks color changes over time, due to the corrosion products, disclosing many lightening or becoming more transparent with time.
In the early Renaissance drawing with a stylus made of lead, silver or other metals, was part of the training of every artist. Leonardo used both lead and silver styli for drawing. The main difference in the use of lead and silver styli derived from the fact that lead will leave a mark on plain paper, whereas silver, being a harder metal, needs a mildly abrasive surface in order to leave a mark [34].

2.2.2 Leadpoint

Leadpoints are an alloy usually with tin, because the pure metals are too soft or pliant. In *Il libro dell'arte* Cennini noted that leadpoint do not necessarily require a prepared ground [15], with the advantage that it is easier to erase the lines if required, but the disadvantage that the tip easily blunts resulting in a coarse line, and, additionally, it can become faded over time. Using leadpoint as the tool is dragged across the surface, metal traces are left behind on the raised fibers of the paper, producing a clean sign, generally easy to be distinguished from other forms of media under magnification. Further, a strong raking light could reveal to the naked eye the iridescent luster to the black particles, which can amalgamate together in quite large soft shapes as the lead point becomes blunt. Traces of black chalk and charcoal appear duller in comparison [12].

2.2.3 Silverpoint

Silverpoint, one of the most common metal points used for drawing, when used on an unprepared paper surface, normally produces no colored but just an indentation. On a prepared surface, fine particles of the metal are taken off and left in the line that has been traced. The stroke, which in addition to the color is characterized by a real scratch on the holder, cannot be erased except by remaking it. This line is usually grey when traced, but it darkens in time and turns to a warmer tone through oxidation or it becomes more transparent over time [12].

2.2.4 Metalpoint grounds

In order to be able to make permanent drawings with the stylus on paper support, it was necessary to incorporate a binder to fix the bone powder to the paper surface. For this purpose, Cennini suggests that the powdered bone be thoroughly ground with lead white pigment, mixed with animal glue (rabbit-skin glue or possibly parchment size) and spread on to the paper with a brush [15]. The grounds can be white or colored by the addition of tinting pigments. Analysis of the grounds in a selection of drawings by Leonardo at Windsor, using Raman spectroscopy, confirms the presence of white particles of calcium phosphate, which can only have come from bones. XRF analysis carried out on a Leonardo drawing at the Metropolitan Museum of Art in New York, found that the ground contained bone black, lead white, vermilion, red lead, azurite and/or blue verditer [13]. The prepared drawing ground of Leonardo sheet considered in this study, not colored, was characterized using the gloss parameter evaluated with the photometric stereo method.

2.2.5 Black chalk

The black chalk was one of the most commonly drawing media of Renaissance artists. Maybe due to this reason Leonardo did not record where he obtained the chalk used, leaving many unresolved issues concerning chalk features and then for a fine appearance reconstruction. As Leonardo's scholars, we will refer to the general features of this material. Natural black chalk is relatively hard when compared with other drawing chalks, pastels, and charcoal. This physical property enables natural black chalk to be sharpened to a very fine yet durable point capable of producing very detailed work [35]. The color of natural black chalk is that of hard coal, varying from black to a cool gray. Strokes made with natural chalks are grainy and irregular and remain on the surface of the paper. Sometimes minuscule scrapes and indentations can be seen, the result of harder inclusions in the point.

The identification of black chalk has sometimes posed difficulties as superficially it can look like charcoal; however, an accurate visual examination allows a correct identification (i.e. an appropriate appearance modeling) [13]. A valuable physical property of natural black chalk is its ability to produce deep rich dark tones. Natural black chalk produces a much deeper black than charcoal. The color of charcoal tends towards a browner or greyer black than that of chalk. The appearance of black chalk dust under magnification is granular and rounded whereas that of charcoal is sharp-edged, angular, plate-like, or splintery. Furthermore, black chalk has a cohesive property that tends to make the particles clustered together: drawn lines of black chalk show the particles clumping and collecting along the edges of fibers where they lie across the path of the stick of chalk as it is dragged across the paper. The effect of the soft charcoal stick on the paper results in an 'explosion' of tiny particles around the drawn line and this scattering of minute fragments of carbon dust is central for the correct recognition [36].

2.2.6 Metalpoint and black chalk appearance behavior

We remark, as first, that appearance behavior of silverpoint and leadpoint are very similar. The main differences are changes in the amplitude and micro shape of the sign on the paper and in the color. Both those parameters are well represented by an accurate color map. Similarly, black chalk perception is very similar to charcoal at real scale, but different at microscale.

For compactness of representation, we decided to use the same appearance model of the paper, just changing reflection and gloss parameters (see paragraph 5.2). This well fit metalpoint behavior. Chalk appearance, instead, could present some inaccuracies in the specular component where falloffs appear broader than those resulting in our rendering. However, the difference is very limited (less than 50 μm) and then inaccuracies appear just at a very small scale, presenting a limited interest for researchers and conservation operators.

Parameters evaluated are gloss, transmission, scattering, and absorption. These were shared for the metalpoint signs. As for paper, the gloss was evaluated using photometric techniques, starting from the segmentation achieved and using a neural network approach. The Refractive index comes from literature due to the difficulty to put in place an efficient examination and the lack of other technical examinations.

For chalk, we referred to the Conservation and Art Materials Encyclopedia Online (CAMEO) [37]. To fit the anisotropic behavior the information material database reports the two values of e =1.486 and w =1.64 -1.66.

For silverpoint, we referred to [38], from which is extracted a value of n = 0.24000. This evaluation has proven to be enough accurate also because there is some circumstantial evidence that the silverpoints in use in Leonardo's workshop in Milan were solid silver [13].

For leadpoint we referred to [39], from which is extracted a value of n = 2.2318. This evaluation is not true accurate as we don't know the recipe of the alloy used by Leonardo. However, at the scale of the human perception, the difference is very limited.

2.3 Iron-gallic ink

Leonardo, usually, perfected his drawings using mostly pen and ink, a common practice in Italian Renaissance drawing [13]. Inks were used 'undiluted' to trace lines, but also diluted with a suitable solvent, generally water, to increase the tonal range of drawings and to create shadows or subtle effects. In this last case, they were generally applied with a brush [40] and the process is termed wash.

Leonardo appears to have exclusively used a quill pen for both writing and drawing. This preference, shared with the other Italian artists, was based on the availability, together with the advantages of suitable length and diameter, the appropriate thickness, flexibility, ability to be sharpened to a point, and resistance to deterioration. Cennini gave precise instructions on how to cut and shape a quill [15].

The Renaissance artist had three main inks available: carbon, iron-gallic, and bistre. Leonardo used iron-gallic ink, the most common type at the age, a spread due to the simplicity of preparation, the fluidity into the writing support and the difficulty to be removed from the surface it was applied on.

Iron-gallic ink is made from tannin or gallotannic acid which is derived from oak galls. When it is combined with ferrous sulfate (green vitriol), a colorless compound, ferrous gallotannate is formed, developing in 7-9 days a black color on exposure to air due to oxidation to ferric gallotannate. The ink ingredients are suspended in a binder consisting of a solution of Arabic gum and water, which increases the medium viscosity favors the ink adhesion to the support and avoids the ink bleeding on the paper. If applied when freshly made, iron-gallic inks can be very pale (e.g. in some part of the *Landscape 1473* drawing). To avoid this problem, it must be left to 'pre-oxidize' and darken before use. As ink ages, it gradually changes from a very dark brown to paler shades, progressively rusty hue and pale orange. This is due to the use of different recipes, and therefore variable materials, concentrations and compositions of chemical substances, which cause very different stability, appearance and degree of damage. Ink with a good balance will end up turning into a rusty brown; an excess of iron sulfate turns the original black ink into a dark rusty-brown color, an excess of tannin into a reddish-brown color [12]. E.g. in the front side of the *Landscape, 1473* colorimetric analysis assigns to the two inks two clearly distinct layers of the drawing, with one of the two inks balanced, and one displaying an excess of iron sulfate [7]. Leonardo refers clearly to the use of this ink for drawing [41].

When light strikes iron-gallic ink, the light is either reflected, transmitted, scattered, or absorbed. Main parameters featuring iron-gallic ink appearance are:

- Diffuse reflectance
- Gloss
- Transmission
- Scattering and absorption.

A first observation concerns the transmission of light that was modeled simply considering the thickness of the ink. Light is assumed to be attenuated by the same factor when crossing the ink layer, independently of its angular distribution (non-orientational model), as in the Clapper-Yule model [42]. After the segmentation from paper and metalpoint using the color map, an evaluation of the lightness was made. The estimate starts from the consideration that higher values of lightness denote lighter thickness and higher transmission. Normalization was achieved according to the direct observation of the ink behavior on the original drawing. The literature reported an accurate measurement of the refraction index of the iron-gallic ink prepared using a recipe of the first half of the 15th century, very similar to those described by Leonardo and Cennini. The resulting refractive index - measured and reported for many frequencies using a spectroscope - is n = 1.35, at a wavelength of 589.3 nm [43]. Finally, the gloss was measured as for chalk, metalpoint, and paper using photometric stereo techniques and producing a gloss map for each pixel sampled.

3 The rendering system

A formally correct approach to drawing materials used by Leonardo requires an accurate selection and customization of the traditional RTR GPU-accelerated graphic pipeline [44], applying principles inferred by Physically Based Rendering (PBR). From the implementation point of view, this results in the need of a scriptable RTR pipeline able to support both an accurate light transport and the Torrance-Sparrow theory for off-specular reflections on micro-faceted surfaces [45].

To speed up the development and avoid porting issues on different platforms, we exploited an existing visualization application taking advantage of its multiplatform and high-quality support, instead of using a specific API graphic in its naïve form, but we customized many components to support our requirements. Mainly, we decided to use the modified version of Torrance-Sparrow by Burley [46] to improve the quality of the result and the efficiency of the pipeline, and shaders were developed to reproduce the correct appearance of drawing materials in which glazing angles and backscattering issues deeply influence resulting spectral behaviors [47].

In the last decade, there have been significant advances in RTR pipelines, and many viewers were developed on existing graphic game engines [48]. We selected the Unity3D rendering engine, capable of supporting PBR using many APIs through its High Definition Render Pipeline (HDRP), a rendering framework tailored on C# scripts and easily customizable on top of Unity3D [49].

The resulting RTR pipeline follows general rendering criteria [50]. Once rasterized, pixels are lightened and colored in the *fragments processing* stage, which is the main core of our novel process, since it was deeply customized to meet the strict requirements needed to visually represent different materials (Figure 2).

In this stage of the pipeline, it is possible to introduce scripts to control how frames are rendered. We developed and implemented features relying on our specific requirements, to ensure precise conformity to:

- *light*, with its actual spectral composition to replicate drawings in an accurate light distribution model;
- *color*, with an accurate simulation to mimic material color appearance under different light directions;
- *surface*, with a precise replica at different meso and micro scales of the paper's surface with a custom implementation of algorithms to simulate the physical behaviors of superficial scattering light.

In section 5 the scripted shaders embedding these features and written in C# will be introduced in detail.

Finally, a Contrast Adaptive Sharpen (CAS) upscaling effect inferred by the HDRP was used to get a feasible antialiasing effect for final high-resolution monitors. The high scalability of the shader developed took explicated our desired portability across different platforms since HDRP in Unity3D uses a dedicated render target allocation system that avoids recurrent reallocation of shaders when resizing the screen. This avoids extra render target allocation when doing dynamic resolution on 4k monitors for example.

The rendering pipeline ends up with the *sampled targeted output*, which covers some technical aspects in terms of final visibility check but most importantly, it considers different output systems to run *ISLe*.

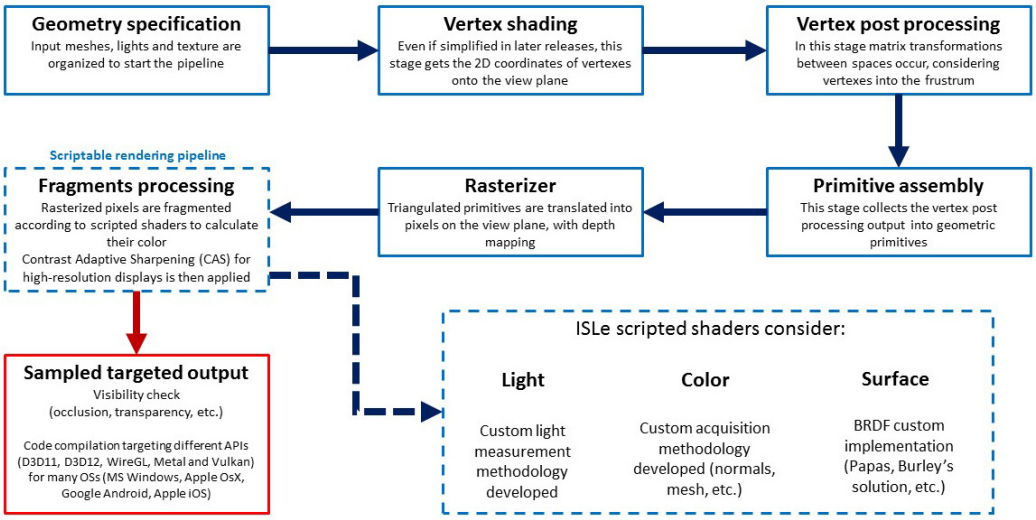

Figure 2: A schematic view of our rendering pipeline, with stages referred to the final visualization in *ISLe*.

The custom pipeline introduced can be compiled to run on many different devices: this is a paramount feature of our *ISLe* system since it is designed to support several kinds of users, from scholars to visitors in museums. Thus, making it available for their OS and hardware environments means to facilitate the system fruition at many levels. Specifically, the last stage in our pipeline exposes frames and translates them into code for different 3D graphics APIs to let *ISLe* be executed on Microsoft Windows, Apple Os X and on mobile devices equipped with hardware running Google Android or Apple iOS (target supported APIs are D3D11, D3D12, WireGL, Metal, and Vulkan).

4 Material modeling

The complex interactions between lights and physical objects, fundamental phenomena to consider in Leonardo's drawings, are usually modeled in CG by the Bidirectional Reflectance Distribution Function (BRDF) [51] that describes, in a quantitative way, the real light reflection considering the entire hemisphere surrounding the light/surface collision point. A detailed introduction of the BRDF theory and its applications, however, can be found in [52]. To model the subsurface dispersion in the homogeneous materials, as e.g. paper, BRDF was extended to the Bidirectional Scattering Distribution Function (BSDF), a quantity that includes the dispersion effects both related to reflection and transmission and essentially consists of the sum of the BRDF and the Bidirectional Transmittance Distribution Function (BTDF). The latter function expresses how light passes through a (semi)transparent surface [53]. This formulation can correctly describe, and it can interpret the correct appearance of paper, metalpoint, ink, and chalk. A correct BTDF modeling starts from the consideration that the appearance of any material is scale dependent. We modeled this fact as in [54], where geometric structures are divided essentially into three different levels:

a. *macrostructure*: the shape and the geometry of the object;
b. *mesostructure*: all those elements still visible with the naked eye but not responsible for the global shape definition of the model. These small details of the surface are e.g. small bumps that cause interreflections and self-shadowing;
c. *microstructure*: it is the microscopical structure not visible to the human eye (e.g. cells, fibers of the paper) that still contributes to the final aspect of the object because it can occlude or deviate light and project shadows and highlights on itself.

The implementation of this structure was accomplished using multitexture techniques [55] with four types of maps: albedo (diffuse), normal, height (surface mesh), and glossiness (specular) applied according to alpha masks. The technique used to generate the albedo map is illustrated in detail in [7]. The alpha-mask maps are

responsible to discern the glossiness values on specific areas according to different materials (see paragraph 3.1). In the next paragraphs, we will focus on three critical features on which the major attention was paid:

a. normal map creation;
b. conversion into mesh surface of the macrostructure (heightmap) extracted from the normal map;
c. shaders development.

4.1 Normal map construction

In our system, we start from a normal map to represent surface orientation and surface heights. In the normal map, the normal vectors are encoded per pixel in the tangent space, so that their vector components are represented as RGB channels scaled between 0 and 255 (given an 8-bit picture). The normal map is used during rendering to calculate the surface shading generated by the mesostructure. The macroscale structure is extracted from the normal map and it is geometrically represented as a mesh.

The mesoscale normal map generation and the macroscale mesh reconstruction are achieved through the application of the photometric stereo technique. Unlike photogrammetry, photometric stereo works extremely well on surfaces with a low amount of details, such as drawings, and it can produce high-resolution normal maps and submillimeter precision surface measurements. Practically we used a customization of the solution developed for paintings in [56] and [57] and implemented in the *4LI-S* software [58].

4LI-S is based on the acquisition of 4 images of the object together with a neutral grey cardboard acquired with different illumination conditions coming from four lights at an angle of 45° with respects to the drawing plane, oriented toward the intersection of the two main orthogonal axes and placed at hours 3, 6, 9 and 12. Furthermore, a glossy sphere is used to precisely identify the direction of the lights.

A first improvement is made on the light decay correction process and the CC process ahead in the pipeline, directly on RAW images before the normal map extraction, using our SHAFT software [10] for CC, and the flat-field method for the light decay correction as in [59]. In this light decay correction procedure, implemented also in *4LI-S*, the four images of the neutral grey cardboard are divided by the relative four images of the drawing captured with the same light conditions. The intensity range of individual pixels in the object images is rescaled between 0 and the mean value of the total individual pixel values of the grey cardboard images before performing the division. Thus, the flattened results would have an intermediate intensity level and no pixels will exceed the pixel values boundaries (the starting intensity range was from 0 to 255 given 8-bit picture). Moreover, the early application of these corrections in the process leads to better overall results, avoiding problems at later stages.

A second improvement concerns the approximation of glossy surfaces into Lambertian surfaces. In the original workflow, the four pictures of drawing are compared and their pixels with the highest and the lowest intensity are excluded to remove potential shadows and highlights. However, this step might cause artifacts in areas with high contrast at albedo level if the surface is already very close to being Lambertian. Thus, we observed that in these cases the exclusion of this step might give better results. Due to this, we introduced a preliminary test to switch on/off the process.

4.1.1 Normal map processing to split macroscale and mesoscale features

Different scale details are obtained with a two steps process from the same normal map:

- splitting of the normal map into two different normal maps with information at a different level of magnitude (i.e. submillimeter and millimetric)
- generation of the mesh with the macroscale details.

To extract macroscale details, we used a map generated by applying a Gaussian blur filter to the normal map calculated by *4LI-S*. In detail, to exclude macroscale features from the original normal map keeping only small details, the blurred map is subtracted to the normal map of a flat surface, and the result is added to the original map, as follows:

$$m = n - (b - f)$$

where m = the normal map with only the mesostructured, n = original normal map with both macroscale and mesoscale features; b = blurred normal map, which is the original normal map with a Gaussian blur filter

applied (the radius of the kernel depends on the size of the details and on the resolution of the image); f = normal map of a flat surface (RGB value equal to 128,128,255 in every pixel, given 8-bit picture).
To avoid typical problems of CG applications that sometimes flatten negative values to zero, the formula can be repeated twice inverting the sign and order of operators the second time (Figure 3). The resulting map presents smoothen out macroscale features and preserved mesoscale asperities (Figure 4).
Regarding the filtering operation, we observed that the bilateral filter [60] gives excellent results, both in the cases with soft and sharp changes of curvature at the macroscale level, but it requires an accurate manual parameter adjustment. The Gaussian blur filter [61], although it presents problems with sharp creases with a rapid and relevant change of direction of the normal vectors - a feature however not present in Leonardo's drawings -, provides more predictable results and is more suitable for automation.

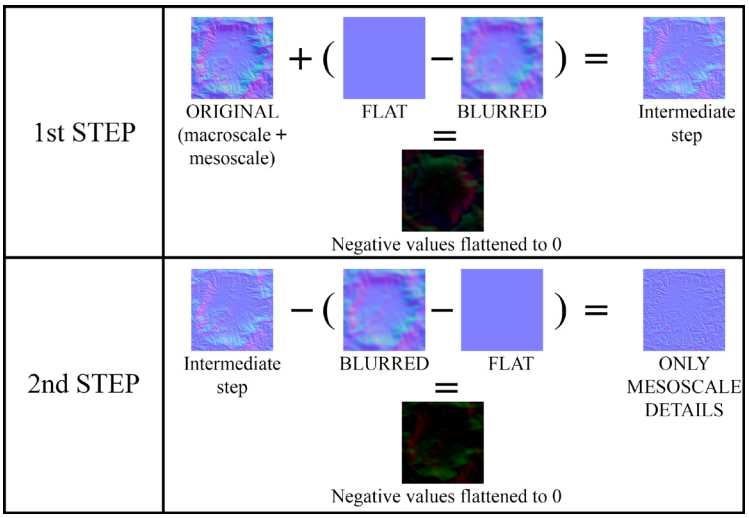

Figure 1: Details extraction from normal maps.

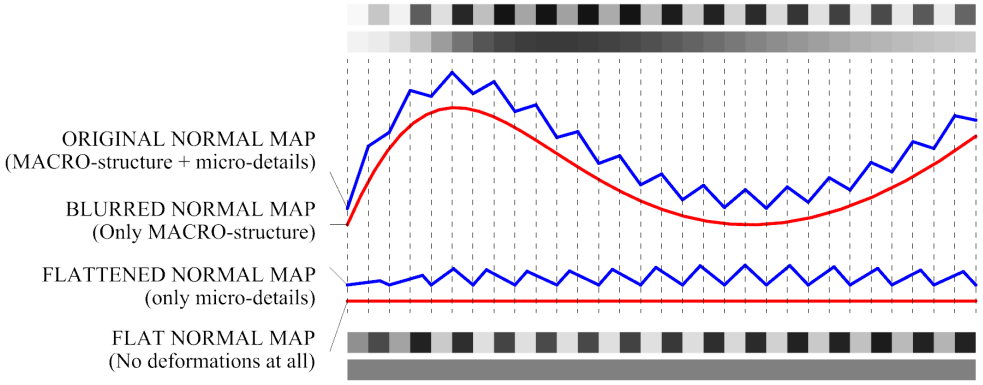

Figure 4: Flattening of the macrostructure.

4.1.2 Mesh construction and error evaluation

The final step is the extraction of the surface mesh. It consists of converting the normal map with only the macroscale features into a surface according to its normal vector orientation, through an algorithm that follows a minimization error rule developed using Grasshopper and its plug-in Kangaroo.
The iterative algorithm deforms a planar surface, with the same ratio of the normal map, into a target mesh surface according to the vectors extracted from the normal map. The solver applies forces to the vertices of the planar mesh based on several geometric constraints and iteratively minimizes the total sum of the weighted squares of all the shifting distances until it reaches an equilibrium configuration according to a

certain tolerance. As additional constraint, we anchor the perimetral points on the XY plane because the perimetral pixels of each picture always capture the table surface, which is known to be planar.
The main problem of this technique is the calibration phase to convert normalized displacement in metrical shifts. In our case, this was achieved by taking two drawings with features (sizes, paper, signs, …) like those of Leonardo and comparing the two mesh surfaces captured with photometric stereo and automatic photogrammetry [62]. Further verification was done comparing specific features of the *Vitruvian Man* exploiting existing measurements on the original paper sheet.
To describe the calibration process at first, we remark that, since the maximum displacement found in the originals is about 4 mm, the maximum error possible is 30 µm that is more than an order of magnitude lower of the displacement considered at the actual scale.
The photogrammetric survey was performed using a Canon EOS 700D camera featuring an 18-megapixel CMOS sensor (4.29 µm pixel size) and equipped with a 60 mm prime lens mounted on the camera yielding to a camera-to-object 0.66 m distance. Given the requirements of micro-meter accuracy for 3D geometry, a 0.058 mm spatial resolution was obtained, corresponding to a photographic scale of 6:1. With such a scale, the Ground Sample Distance (GSD) of the images is about 0.04445 mm/px, the same as the photometric stereo. A dataset of 44 pictures was processed with the software Agisoft Metashape. To avoid projecting coupling between interior and exterior orientation parameters due to the flat shape of the object, a proper camera network was planned, including convergent and rotated images. This step is mandatory if reliable results are expected and to avoid degradation of object points precision [63].
At the end of the bundle adjustment, the automatic tie point extraction on the paper surface achieved an RMS of image observations of 0.403 pixels and a mean key point size of 2.67998 px. A dense image matching procedure was run in Metashape with a sampling interval of 0.12 mm producing a dense point cloud of 23.5 million points, and a model of about 800,000 vertices.
To evaluate the accuracy of this process we compared the surface obtained by photometric stereo and that from photogrammetry in Cloud Compare. To avoid the boundary conditions accuracy problems at the drawing scale and the typical problems of relevant noise at the macroscale of the automatic photogrammetry, we compared the entire drawing acquired with both systems as well as smaller square patches of different size (100x100 mm and 50x50 mm) and located in different positions of the drawing. For the entire drawing the average Gaussian mean is 5 µm and the standard deviation is 0.95 mm, for the patches of 100x100mm size the average Gaussian mean is 0.02 mm and the standard deviation is 0.20 mm. (Figure 5).

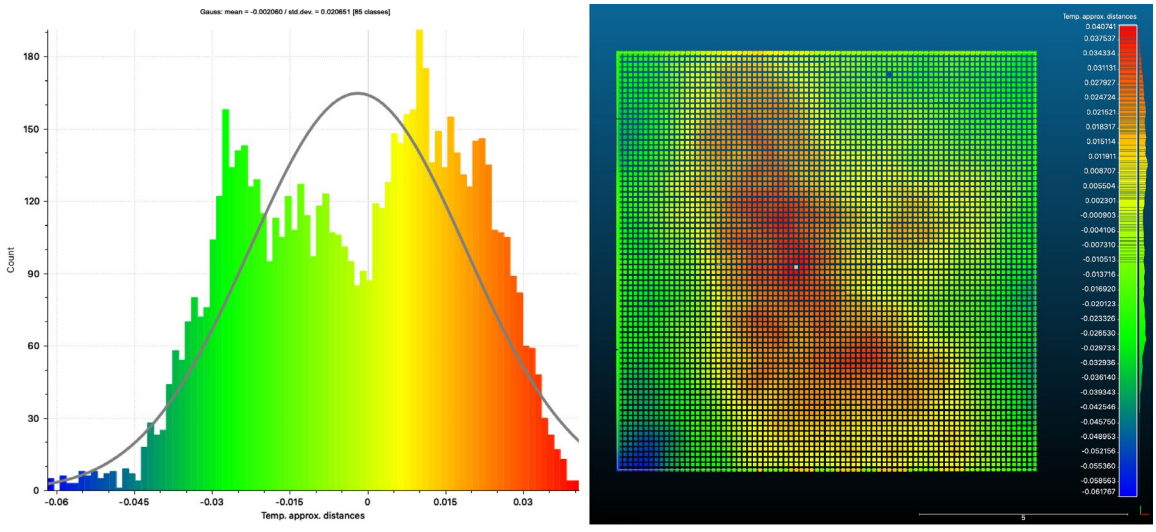

Figure 5: comparison between the mesh surface generated with photogrammetry and the mesh surface generated with photometric stereo of a 17th-century drawing (size 450x300mm) for the patch size of 100x100mm.

4.1.3 Process criticalities & accuracy

It was observed that the 4LI-S guarantees high precision at the mesostructure level. However, it is less accurate when the map is used to reconstruct the macrostructure (i.e. large-scale deformations of the paper). The macrostructure error is mainly generated by the following factors:

a. non-uniform correction of the light decay in post-production due to small changes in the boundary conditions during the capture phase.
b. non-perfect light emitter. The light emitter should be a point at infinite distance to guarantee parallel rays, in this way the intensity level measured on individual pixels would correspond exactly to its orientation with regards to the light emitter. The fact that the light emitter is closer to the drawing causes the rays to be convergent in one point. This problem is trivial at mesoscale why it is more accurate than macroscale.
c. the classical photometric stereo also assumes Lambertian surfaces with perfect diffuse reflection. However, this assumption is not completely valid in the case of paper sheets because it is not a perfect isotropic Lambertian surface. This generates a small local error but at macroscale it can cause a shift of the inclination values of the vectors normal to the surface even by several degrees. Even if 4LI-S applies artificial correction for that, it is not 100% accurate and it is based on assumptions independent from the material surface properties of the captured object.
d. the components of the normal vector are discretized on a scale of 255 values (given 8-bit pictures). This implies small approximations which might also contribute to add small errors locally and possible significant error if extended to the whole pixel array.

We described the process to improve a. and c.; point b. could be partially solved by correcting the direction of the light angle pixel by pixel according to the distance from the point on the drawing to the light emitter, this would require to precisely measure the distance of light and not only its angle; point d. can be solved by working with 16-bit pictures or remapping the RGB values between 0 and 1 float numbers with high decimal accuracy and remap them back to 8- or 16-bit space once the calculation is finished. We have not adopted these measures because in our case it was observed that errors were negligible.

4.2 Shaders authoring

As we observed, the BSDF model formulation used for paper is a superset of the BSDF formulation for other materials with minimal errors, then, for implementation slenderness, we used the same shader with different parameters and maps. To better understand we describe accurately the paper appearance model and its implementation and just parameters and main features of the other materials, considering that in practice they have a very limited thickness, and then they mainly add color and highlights to the paper surface.

4.2.1 The paper shader

In recent work, Papas et al. [32] introduced an accurate model of paper's BRDF, with the formulation of a BSDF that considers transmission and diffusion of light given from a scientifically verified observation on how paper is highly dispersive [64]. This expression could be used also for Leonardo's drawings, modeling paper as an optically thick material that entails light behaviors given by the combination of many effects: subsurface dispersion, mirror reflection, retro-reflection, surface glossiness, and transmission. Thus, paper behavior is reconstructed using a BSDF representation exploiting three components:

- a reduced version of the multi/layered model of Donner and Jensen [65];
- the single dispersion theory model [66];
- the microfacets model for surface reflections and refractions as in [53].

In detail, for what concerns the microfacet model, if superficial reflections scatter from the light incoming vector l and the outgoing direction view v, as the microfacet model postulates, a small portion of the surface (a microfacet) with an equiangular normal direction between l and v must exist. This 'half-vector' is represented as the micro-surface normal and it is evaluated as $h = l + v$. The general mathematical formulation of a micro-faceted model for isotropic materials is represented by:

$$f(l,v) = \frac{c_{diff}}{\pi} + \frac{F(l,h)G(l,v,h)D(h)}{4(n \cdot l)(n \cdot v)}$$

where:

- c_{diff} = light portion diffused by albedo;
- *F(l,h)*= Fresnel reflectance; a term that calculates the fraction of light reflected by an optically flat surface. Its value depends on two factors: the angle between the light vector and the normal surface and the refractive index of the material. Since the refractive index can vary over the entire visible spectrum, the Fresnel reflectance is a spectral quantity;
- *G(l,v,h)* = statistical amount of microfacets occluded or shaded by the surface shape when hit by light along the *l* direction toward the *v* view vector, considering the *h* normal for every facet. Our approach to mimic paper's micro facets considers also inter-reflections (light bounces amid micro facets before reaching the viewer);
- *D(h)* = normal distribution function for every micro facet; *D(h)* expresses the number of microfacets with normal equal to *h* and determines the size, brightness, and shape of the specular illumination;
- $4(n \cdot l)(n \cdot v)$ = correction factor that considers quantities that must be transformed between the local space of the microfacets and the global one of the entire surface.

As demonstrated by [32] for rough surfaces like matte paper, as that used by Leonardo for his drawings, the Fresnel transmission equation seems not to be an appropriate solution. Starting from the measurements made, they found that the transmission is correlated to the direction of the incident light, to the refractive index, and the roughness. To consider this phenomenon an attenuation function is introduced. Instead of their formulation, accurate but computationally expensive to be used in RTR, we exploited the BSDF implementation provided by the Walt Disney Animation Studios [67], that, calculating twice the Fresnel refraction - both for incoming and outgoing light that scatters from the paper's surface - to preserve Helmholtz's principle of reciprocity. The Fresnel refraction was calculated introducing the Schlick approximation [68], which expresses the grazing retro-reflection response by passing to a specific value determined by the roughness instead of a null value:

$$F_{Schlick} = F_0 + (1 - F_0)(1 - cos\theta_i)^5$$

where F_0 constant represents the reflectance specular to the normal incidence, which is achromatic for dielectrics and chromatic for metals. The current value depends on the index of refraction. Specular reflection comes from the microfacets and therefore F depends on θ_i, which is the angle between the light vector and the micronormal (i.e. the semi-vector h). The error introduced by this approximation is significantly smaller than that due to other factors, allowing to consider Fresnel deficiencies in presence of opaque paper, as [32], improving the overall original non-natural response to grazing light. To introduce terms that evaluate subsurface scattering, the diffuse lobe was refactored evaluating directional microsurface effects and non-directional subsurface effects (i.e. Lambertian). Then the Lambertian portion of the diffuse lobe was replaced with a diffusion model together with a volumetric dispersion model. This technique preserves the effects of the microsurface, letting the diffusion model converge to the same result as the diffused BRDF when its dispersion distance is small enough. To allow the light exchange of the Lambertian diffusion with the subsurface scattering, while keeping the Fresnel factors for rough surfaces and retro-reflective gains, the diffuse reflection model was refactored as in [46]. As in [53] to evaluate *G(l,v,h)* is used the Smith's solution and to compute *D(h)* is employed the multi-dispersion anisotropic GGX. This last factor, however, was written in Heitz's formulation [69].

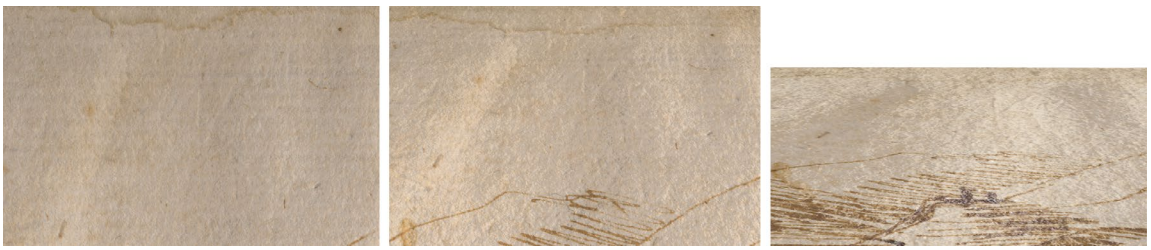

Figure 6: Paper shader RTR of the Landscape 1473 drawing with different light positions: zenithal (left), at 45° (center), raking (right).

Finally, this scheme was implemented in the Unity3D environment beginning from what is extensively reported in [70]. In Figure 6 there is the result and in figure 7 is reported the shader graph of the paper of the *Vitruvian Man* drawing referring to the Unity3D's HDRP libraries.

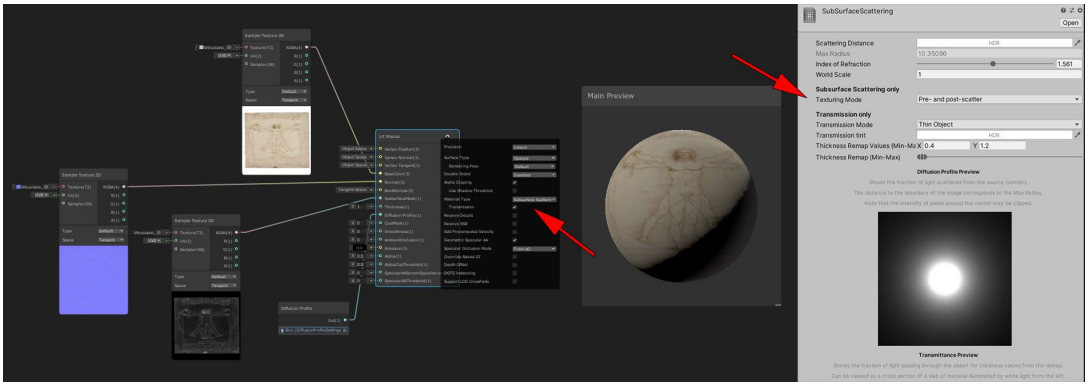

Figure 7: The schematic shader features in the Vitruvian Man ISLe model: the paper introduces the Walt Disney Animation Studios' approximation with a double calculation for the Fresnel reflectance.

4.2.2 The iron-gallic ink, metalpoint and black chalk shaders

The strategy used for the tracing materials is to use specific shaders into accurately locate areas on the paper where the specific instrument is used. In the compiled paper shader, a transparency mask channel was generated exploiting our accurate segmentation technique and used to bound areas where is assigned the new shader to recreate the ink (metalpoint, chalk, ...) signs, as documented in Figure 8. The result is in Figure 9. The process to generate shaders for drawing instruments used by Leonardo is similar and it exploits the paper shader that is adapted just editing parameters and maps. Measurements and datasets collected analyzing real drawings by Leonardo provided us with the necessary information to deal with these parameters, as described in paragraphs 3.2, 3.3.

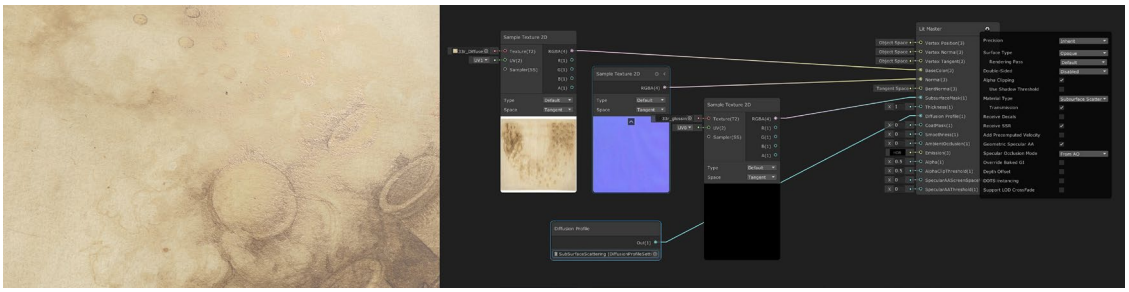

Figure 8: Different inks and watercolors as represented by our shader, which simulates iron gallic ink, metalpoint, and paper for the Two mortars launching explosives ISLe model (left). The shader graph showing maps and subsurface scattering profile connections as coded in our custom shader (right).

Figure 9: Ink shader RTR of the Landscape 1473 drawing with different light positions: zenithal (left), at 45° (center), raking (right).

E.g. to mimic iron-gallic ink the shader was prepared to replicate light scattering on the thin ink's layer, considering its diffuse reflectance, its glossiness, evaluating the scattering and absorption of light as it is transmitted into the material. Our shader implements anisotropic multi scattering GGX for the ink's rendering pipeline, leading to the more realistic effect consisting of rougher traits that are not simply darker but more saturated and translucent, like the real material. The subsurface scattering of light is replicated, anew, using the BSDF described in [46] adding an attenuation by a constant factor when passing through the ink layer, related to its angular orientation.

5 RTR quality evaluation

In order to assess the potential and critical issues of the application, and to collect any suggestions for further developments or implementations two different types of instruments were used:

a. Evaluation of the success against the large audience of exhibitions visitors,
b. Evaluation of the quality by professional operators of conservation and museums field and/or Leonardo works and drawings (art historians, conservators, restorers, museum services).

The evaluation of the positive or negative perception of the audience was measured by the number of visitors in the exhibitions held:

- *Perfecto e virtuale – l'Uomo Vitruviano di Leonardo*, at Centro Studi Vitruviani in Fano (Italy) 24 October 2014 - 6 January 2015, more than 10,000 visitors, without any original material;
- *Leonardo in Vinci, at the origin of the genius*, at Museo Leonardiano in Vinci (Italy) 15 April 2019 - 6 January 2020, more than 140,000 visitors;
- *Leonardo, drawing anatomy*, at Museum of Palazzo Poggi in Bologna (Italy) 23 November 2019 - 6 February 2020, more than 12,000 visitors, without any original material.

The evaluation of quality by a group of experts who had the opportunity to use the application was carried out with a questionnaire. It consists of several sections and subsections: one related to more purely technical aspects of the application, another dedicated to more subjective assessments, and one more dedicated to suggesting any developments or implementation to the application, useful for its use in different areas.
The feedback showed a high level of user satisfaction regarding the qualitative and perceptive characteristics of the digital artifact reproduced with *ISLe* (i.e. interacting with the digital copy of an ancient drawing, as if it were in your hands, or the possibility of compare front and back of a drawing), the possibility of analyzing the graphic characteristics of the media used for the execution of the drawing (i.e. black stone, metal or blind tip, holes, ink, watercolor, etc.), or the characteristics and/or chromatic differences of the artwork due to the use of different media, the characteristics of the support (e.g. paper) on which the drawing was made, or the possibility of analyzing the conservation interventions suffered by the drawing.
Particularly significant seems to be the results deriving from the operational possibilities in support of the interviewees' work, which shows that *ISLe* offers or could offer (Figure 10 - left):

a. always having a reproduction of the drawing available, without the limitations due to the correct rules of conservation of the drawing
b. cross-referencing multiple information deriving from different analysis techniques
c. implementing thematic displays (e.g. by emphasizing details, increasing lighting contrast and/or intensity, or grazing light, etc.)
d. comparing reproductions of the drawing at different times (e.g. before, during and after restoration)
e. zooming freely and interacting simultaneously with the direction of the light source.

Regarding the use of *ISLe*, it emerges that the greatest benefits could be the comparative analysis, in the study of drawings up to the conservation and documentation of artifacts (Figure 10 – right). Furthermore, the results on the more purely subjective evaluations are positive, such as curiosity or interest, as fostered by *ISLe* in studying and observing a drawing.
The collected answers also show how the application would present (at least potentially) a wide versatility of use in different areas, not only in an exhibition and/or museum context, but also for learning, studying dissemination, and entertainment. Similarly, the application was perceived as suitable for all users, but most of the interviewees highlighted how *ISLe* offers to observe, enjoy and understand the masterpieces with the

help of additional tools to support specific user groups. Some of the possible implementations suggested by interviewed scholars concern aspects related to the improvement of the user interface. Other suggestions concern the possibility of simultaneous comparison of the front and the back of the drawing, the possibility of making direct measurements, the overlapping of thematic maps, or of combining images deriving from the use of electromagnetic radiation at different wavelengths and/or transmitted light illumination.

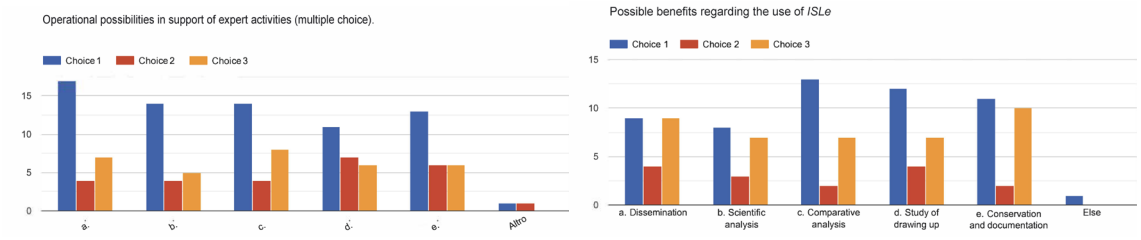

Figure 10: Questionnaire feedback: operational possibilities in support of expert activities (left); possible benefits regarding the use of ISLe (right).

6 Conclusions

The paper presented the RTR system at the ground of the *ISLe* application, a solution for the visualization 'as in your hand' and able to 'show what you do not see' in the digital surrogate of ancient drawings. In detail, we illustrated the implementation for Leonardo da Vinci's drawings that represent a landmark in the 15th and 16th-century fine art drawing because they have greater complexity and more onerous requirements than all other Renaissance paper graphic works.

The design and implementation of the *ISLe* rendering system was the result of the integrated work of a team of experts with our working group, and it is built on already consolidated elements and libraries and grounded on a robust, popular and rich low-cost rendering engine but a massive effort has been put in place to provide access to high-quality visualization coupled with rendering times compatible with an easy RTR interaction. The system has been released progressively after years of intense work, to well characterize the rendering behavior of paper and drawing instruments.

Although the design of the system has been strongly tailored to the peculiar and complex case of Leonardo's drawing, the main goal of this initiative consisted of sketching the outline of a generic system to be used to support study, conservation, and dissemination activities concerning fine art drawings.

The experience with Leonardo's drawing was quite successful. Both the impressive number of visitors at the exhibitions and the results of a questionnaire submitted to sector operators show an appreciation much higher than expected. It opens now a new goal, the design of a cloud-based platform that should support the easy creation of a new visualization context for any drawing able to offer the same functionalities presented in this paper, or in other words, should be customized and offered to the users in an unattended manner (without ICT staff strongly involved in the customization of the RTR system). This could be one of the services of an infrastructure supporting Heritage Science and could be interconnected to other services.

Other directions for future work could be the support for drawings larger than A3 paper sheet and the growth of the material library to other graphic techniques. Finally, other future works were proposed by users and are reported in section 6.

ACKNOWLEDGMENTS

We thank all the institutions that gave us access to the Leonardo drawing and the operators that helped us in the works of drawing acquisition, in particular in the person of Annalisa Perissa Torrini, Eike Schmidt, Laura Donati, Roberto Palermo, Roberta Barsanti, Mons. Federico Gallo, Mons. Alberto Rocca, Fabio Cusimano. The work was accomplished with the technical support of: FOWA, Hasselblad, Relio, Rencay.

REFERENCES

[1] Martin Kemp. 2006. *Leonardo da Vinci - The Marvellous Works of Nature and Man*. Oxford University Press, New York, NY.

[2] Carmen C. Bambach. 2013. Il Volume XXXIV di "Raccolta Vinciana". *Raccolta Vinciana* 35, 253-278.
[3] James A. Ferwerda and Benjamin A. Darling. 2013. Tangible Images: Bridging the Real and Virtual Worlds. In *CCIW 2013 proceedings. Lecture Notes in Computer Science*, 7786. Springer, Berlin, Heidelberg, 13-24. DOI: https://doi.org/10.1007/978-3-642-36700-7_2
[4] Lieve Watteeuw, Hendrik Hameeuw, Bruno Vandermeulen, Athena Van der Perre, Vanessa Boschloos, Luc Delvaux, Marc Proesmans, Marina Van Bos and Luc Van Gool. 2016. Light, shadows and surface characteristics: the multispectral Portable Light Dome. *Appl. Phys. A* 122, 976 (2016), 7 pages. DOI: 10.1007/s00339-016-0499-4
[5] Marco Gaiani, Cristiana Corsi, Marzia Faietti, Ilaria Rossi and Massimo Zancolich. 2011. An unified, fast and low cost workflow for fine art drawing collections acquisition. In *Colour and Colorimetry Multidisciplinary Contributions*, VIIB, Maggioli Editore, Rimini, Italy, 260-267.
[6] Marco Gaiani, Fabrizio I. Apollonio, Paolo Clini. 2015. Innovative approach to the digital documentation and rendering of the total appearance of fine drawings and its validation on Leonardo's Vitruvian Man. *Journal of Cultural Heritage*, 16, 6 (2015), 805-812. DOI: https://doi.org/10.1016/j.culher.2015.04.003.
[7] Marco Gaiani, Fabrizio Ivan Apollonio, Giovanni Bacci, Andrea Ballabeni, Marco Bozzola, Riccardo Foschi, Simone Garagnani, Roberto Palermo. 2019. Vedere dentro i disegni. Un sistema per analizzare, conservare, comprendere, comunicare i disegni di Leonardo. In *Leonardo a Vinci. Alle origini del genio*, Roberta Barsanti (Eds.). Giunti Editore, Milano, Italy, 207-240.
[8] Jassim Happa, Tom Bashford-Rogers, Alexander Wilkie, Alessandro Artusi, Kurt Debattista, Alan Chalmers. 2012. Cultural Heritage Predictive Rendering. *Computer Graphics Forum*, 31 (2012), 1823-1836. DOI: https://doi.org/10.1111/j.1467-8659.2012.02098.x.
[9] Lindsay MacDonald. 2010. The limits of resolution. In *Proceedings of BCS Conference on Electronic Visualisation and the Arts (EVA)*, 149-156.
[10] Marco Gaiani, Andrea Ballabeni. 2018. SHAFT (SAT & HUE Adaptive Fine Tuning), a new automated solution for target-based color correction. In *Colour and Colorimetry Multidisciplinary Contributions*, XIVB, Maggioli Editore, Rimini, Italy, 69-80.
[11] Janet Ambers, Catherine Higgitt and David Saunders (eds). 2010. *Italian Renaissance Drawings: Technical Examination and Analysis*. Archetype Publications, London.
[12] Carlo James. 2010. *Visual identification and analysis of old master drawing techniques*, Olschki, Florence.
[13] Alan Donnithorne. 2019. *Leonardo da Vinci. A Closer Look.* Royal Collection Trust, London.
[14] Michel Menu (Eds.). 2014. *Leonardo da Vinci's Technical Practice: Paintings, Drawings, and Influence*. Hermann, Paris, France.
[15] Cennino Cennini. 2009. *Il libro dell'Arte*. Franco Brunello (Eds.), Neri Pozza Editore, Vicenza, Italy.
[16] Dard Hunter. 1947. *Papermaking: The History and Technique of an Ancient Craft*. Dover, New York.
[17] Loretta Salvador. 2009. *Tecniche, stato conservativo e intervento di restauro*. In *Leonardo L'uomo vituviano fra arte e scienza*. Annalisa Perissa Torrini (Eds). Marsilio, Venezia, 57-67.
[18] Adriano Mosca Conte, Olivia Pulci, Maria Cristina Misiti, Joanna Lojewska, Lorenzo Teodonio, Claudia Violante and Mauro Missori. 2014. Visual degradation in Leonardo da Vinci's iconic self-portrait: A nanoscale study. *Appl. Phys. Lett.* 104, 224101 (2014). DOI: https://doi.org/10.1063/1.4879838.
[19] Martin A. Hubbe, Joel J. Pawlak and Alexander A. Koukoulas. 2008. Paper's appearance: a review. *BioResources* 3, 2, 627-665.
[20] Ramin Farnood. 2009. Review: Optical properties of paper: theory and practice. In *Advances in Pulp and Paper Research*, Oxford 2009. FRC, Manchester, UK (2018), 273–352.
[21] Jens Borch, M. Bruce Lyne, Richard E. Mark, Charles Habeger. 2001. *Handbook of Physical Testing of Paper*, Vol. 2, CRC Press, Boca Raton, USA.
[22] Craig Leising. 2010. *Paper surface roughness with 3D profilometry.* Irvine, USA. http://nanovea.com/App-Notes/paperroughness.pdf. Accessed on April 2020.
[23] Robert J. Woodham. 1980. Photometric Method For Determining Surface Orientation From Multiple Images. *Opt. Eng.* 19, 1, 191139 (1980). DOI: https://doi.org/10.1117/12.7972479.
[24] Shoji Tominaga and Norihiro Tanaka. 2008. Spectral Image Acquisition, Analysis, and Rendering for Art Paintings. *Journal of Electronic Imaging* 17, 4, 13. DOI: https://doi.org/10.1117/1.3036180.
[25] Takayuki Hasegawa, Norimichi Tsumura, Toshiya Nakaguchi and Koichi Iino. 2011. Photometric Approach to Surface Reconstruction of Artist Paintings. *Journal of Electronic Imaging* 20, 1, 11.

[26] Jiaping Wang, Shuang Zhao, Xin Tong, John Snyder and Baining Guo. 2008. Modeling Anisotropic Surface Reflectance with Example-Based Microfacet Synthesis. *ACM Transactions on Graphics* 27, 3, 9 pages. DOI: https://doi.org/10.1145/1360612.1360640.
[27] DARPA. 1988. *Neural Network Study*, Lexington, M.I.T. Lincoln Laboratory MA. https://s3.amazonaws.com/arena-attachments/2618226/4497a1ae3a5e18d1d9e90a7748c1f9b9.pdf. Accessed on April 2020.
[28] Martin T. Hagan and Mohammed B. Menhaj. 1994. Training feed-forward networks with the Marquardt algorithm. In *IEEE Transactions on Neural Networks*, 5, 6, 989–993. DOI: 10.1109/72.329697.
[29] Pul Kubelka. 1948. New contributions to the optics of intensely light-scattering materials, Part I, *J. Opt. Soc. of Am.* 38, 5, 448–457.
[30] Anthony M. Scallan, and Jens Borch. 1972. An interpretation of paper reflectance based upon morphology. 1. Initial considerations. *Tappi*, 55, 4, 583-588.
[31] Markku Leskelä. 1993. Model for the optical properties of paper. Theory. *Paperi ja Puu* 75, 683-688.
[32] Marios Papas, Krystle de Mesa, Henrik Wann Jensen. 2014. A Physically-Based BSDF for Modeling the Appearance of Paper. *Computer Graphics Forum*, 33, 4, 133-142. DOI: 10.1111/cgf.12420
[33] Marco Peccianti, Renato Fastampa, Adriano Mosca Conte, Olivia Pulci, Claudia Violante, Joanna Łojewska, Matteo Clerici, Roberto Morandotti and Mauro Missori. 2017. Terahertz absorption by cellulose: application to ancient paper artifacts. *Phys. Rev. Applied*, 7, 064019. DOI: 10.1103/PhysRevApplied.7.064019.
[34] Letizia Montalbano, Cecilia Frosinini, Alain Duval, Hélène Guicharnaud, Giuseppe Casu. 2002. Metal-point drawings: International studies on the artistic technique and identification of metal-point line. In *ICOM 13th triennial meeting*, ICOM-CC, London, UK, 609-614.
[35] Timothy David Mayhew, Margo Ellis and Supapan Seraphin. 2010. Natural black chalk in traditional old master drawings. *Journal of the American Institute for Conservation*, 49, 2, 83-95. www.jstor.org/stable/41320440. Accessed 25 Apr. 2020.
[36] Jenny Bescoby, Judith Rayner and Satoko Tanimoto. 2010. Dry drawing media. In *Italian Renaissance Drawings: Technical Examination and Analysis*, Janet Ambers, Catherine Higgitt, David Saunders (Eds.), Archetype Publications, London, UK, 39-56.
[37] http://cameo.mfa.org/wiki/Chalk Accessed 25 Apr. 2020.
[38] Philip B. Johnson and Robert W. Christy. 1972. Optical constants of the noble metals. *Phys. Rev. B 6*, 4370-4379. DOI: https://doi.org/10.1103/PhysRevB.6.4370.
[39] Alexander I. Golovashkin and G. P. Motulevich. 1968. Optical properties of lead in the visible and infrared spectral ranges, *Soviet Physics JETP* 26, 881-887.
[40] Giovanni Verri, Satoko Tanimoto and Catherine Higgitt. 2010. Inks and washes. In *Italian Renaissance Drawings: Technical Examination and Analysis*, Janet Ambers, Catherine Higgitt, David Saunders (Eds.), Archetype Publications, London, UK, 57-76.
[41] Leonardo da Vinci, Codex Forster, III, f. 39v.
[42] Frank R. Clapper and John A.C. Yule. 1953. The Effect of Multiple Internal Reflections on the Densities of Halftone Prints on Paper. *J. Opt. Soc. Am.* 43, 600–603.
[43] Andrea Taschin, Paolo Bartolini, Jordanka Tasseva, Jana Striova, Raffaella Fontana, Cristiano Riminesi and Renato Torre. 2017. Drawing materials studied by THz spectroscopy. *ACTA IMEKO*, 6, 3, 12-17.
[44] Tomas Akenine-Möller, Eric Haines and Naty Hoffman. 2018. *Real-Time Rendering*. 4th ed. Fourth edition. Taylor & Francis, CRC Press, Boca Raton, FL. DOI: https://doi.org/10.1201/b22086.
[45] Kenneth E. Torrance and Ephraim M. Sparrow. 1967. Theory for off-specular reflection from roughened surfaces. *Journal Optical Soc. America*, 57, 9, 1105-1114.
[46] Brent Burley. 2015. Extending Disney's Physically Based BRDF with Integrated Subsurface Scattering. In *SIGGRAPH '15 Courses*, ACM, New York, 2015, Article 22.
[47] Gabriyel Wong and Jianliang Wang. 2017. *Real-Time Rendering: Computer Graphics with Control Engineering*, Taylor & Francis, CRC Press, Boca Raton, Fl.
[48] David H. Eberly. 2015. *3D Game Engine Design: A Practical Approach to Real-Time Computer Graphic*s. Taylor & Francis, CRC Press, Boca Raton, Fl.
[49] Sebastien Lagarde. 2018. *The High Definition Render Pipeline: Focused on visual quality*. Available online: https://blogs.unity3d.com/2018/03/16/the-high-definition-render-pipeline-focused-on-visual-quality/ Accessed 25 Apr. 2020.
[50] Matt Pharr, Wenzel Jakob and Greg Humphreys. 2016. *Physically Based Rendering: From theory to Implementation*, Morgan Kaufmann Publishers.

[51] Fred E. Nicodemus. 1965. Directional reflectance and emissivity of an opaque surface. *Applied Optics*, 4,7, 767-775.
[52] Dar'ya Guarnera, Giuseppe Claudio Guarnera, Abhijeet Ghosh, Cornelia Denk, Mashhuda Glencross. 2016. BRDF Representation and Acquisition. *Computer Graphics Forum*, 35, 2, 625-650. DOI: https://doi.org/10.1111/cgf.12867.
[53] Bruce Walter, Stephen R. Marschner, Hongsong Li and Kenneth E. Torrance. 2007. Microfacet models for refraction through rough surfaces. In *Proceedings of the 18th Eurographics conference on Rendering Techniques.* Eurographics Association, 195–206.
[54] Stephen H. Westin, James Arvo and Kenneth E. Torrance. 1992. Predicting reflectance functions from complex surfaces. In J.J. Thomas (Ed.), 1992. *Proceedings of the 19th annual conference on Computer graphics and interactive techniques* (SIGGRAPH '92), ACM, New York, NY, 255-264.
[55] Cindy M. Goral, Kenneth E. Torrance, Donald P. Greenberg and Bennett Battaile. 1984. Modeling the Interaction of Light Between Diffuse Surfaces. In *Proceedings of the 11th Annual Conference on Computer Graphics and Interactive Techniques* (SIGGRAPH '84), ACM, New York, NY, 213-222.
[56] Brittany D. Cox and Roy S. Berns. 2015. Imaging artwork in a studio environment for computer graphics rendering. In *Proceeding of SPIE-IS&T Measuring, Modeling, and Reproducing Material Appearance 2015*. Vol. 9398, 939803 (2015). DOI: https://doi.org/10.1117/12.2083388
[57] Brittany D. Cox and Roy S. Berns. 2015. Using Maya to create a virtual museum. In *Proceedings of IS&T Archiving Conference*, 51-55.
[58] https://www.rit.edu/cos/colorscience/mellon/software.php Accessed 25 Apr. 2020.
[59] Joel Witwer and Roy S. Berns. 2015. Increasing the Versatility of Digitizations through Post-Camera Flat-Fielding. In *Proceedings of IS&T Archiving Conference*, 110-113.
[60] Sylvain Paris, Pierre Kornprobst, Jack Tumblin and Frédo Durand. 2009. Bilateral Filtering: Theory and Applications. *Foundations and Trends in Computer Graphics and Vision*, 4, 1, 1-73.
[61] Raphael C. Gonzalez, Richard Woods. 1992. Digital Image Processing, Addison-Wesley, Boston, MA.
[62] Fabio Remondino, Alessandro Rizzi, Luigi Barazzetti, Marco Scaioni, Francesco Fassi, Raffaella Brumana and Anna Pelagotti. 2011. Review of Geometric and Radiometric Analyses of Paintings. *The Photogrammetric Record,* 26, 439-461. DOI:10.1111/j.1477-9730.2011.00664.x
[63] Dante Abate, Fabio Menna, Fabio Remondino and Maria Grazia Gattari. 2014. 3D painting documentation: evaluation of conservation conditions with 3D imaging and ranging techniques. *ISPRS ARCHIVES,* XL-5, 1-8. DOI: 10.5194/isprsarchives-XL-5-1-2014.
[64] Frederick O. Bartell, Eustace L. Dereniak, William L. Wolfe. 1980. The theory and measurement of bidirectional reflectance distribution function (BRDF) and bidirectional transmittance distribution function (BTDF). In *Proceedings of SPIE,* Vol. 257, pp. 154-160.
[65] Craig Donner, Henrik Wann Jensen. 2005. Light diffusion in multi- layered translucent materials. In *ACM Trans. Graph.* 24, 3, 1032–1039. DOI: 10.1145/1073204.1073308
[66] Pat Hanrahan, Wolfgang Krueger. 1993. Reflection from layered surfaces due to subsurface scattering. In *Proceedings of the 20th Annual Conference on Computer Graphics and Interactive Techniques* (SIGGRAPH 93), ACM, New York, NY, 165–174.
[67] Brent Burley. 2012. Physically-based shading at Disney, course notes. In *SIGGRAPH '12 Courses*, ACM, New York, 2012, Article 10.
[68] Christophe Schlick. 1994. An Inexpensive BRDF Model for Physically Based Rendering. *Computer Graphics Forum,* 13, 3, 233–246.
[69] Eric Heitz. 2014. Understanding the masking-shadowing function in microfacet-based BRDFs. *Journal of Computer Graphics Techniques*, 3, 2, 32-91.
[70] Claudia Doppioslash. 2018. *Physically Based Shader Development for Unity 2017*, Apress.